Aberrant DJ-1 expression underlies L-type calcium channel hypoactivity in dendrites in tuberous sclerosis complex and Alzheimer's disease

Farr Niere[1,2†], Ayse Uneri[1†], Colin J. McArdle[1], Zhiyong Deng[1], Hailey X. Egido-Betancourt[1], Luisa P. Cacheaux[1], Sanjeev V. Namjoshi[1], William C. Taylor[1], Xin Wang[3], Samuel H. Barth[1], Cameron Reynoldson[1], Juan Penaranda[1], Michael P. Stierer[1], Chelcie F. Heaney[1], Suzanne Craft[4], C. Dirk Keene[5], Tao Ma[3,1], and Kimberly F. Raab-Graham[1*]

List of Supplementary Information:

Supplementary Figures 1-14

Extended Materials and Methods

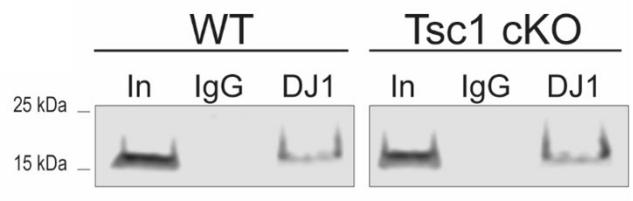

Figure S1: Western blot confirmation of RNA-Immunoprecipitation (R-IP) of DJ-1. Western blot of 25% of precipitate ran on 10% SDS-PAGE, showing DJ-1 is successfully immunoprecipitated from WT and Tsc1 cKO cortical lysates, while the negative control, IgG, is void of DJ-1 bands as expected.

		WT			*Tsc1* cKO			WT vs TSC IP
		mean	SEM	p-value	mean	SEM	p-value	p-value
cacna1c	DJ-1	0.05151	± 0.02971	0.16	0.9502	± 0.2896	0.03	0.03
	IgG	0.001112	± 0.0007232		0.003339	± 0.001648		
cacna2d2	DJ-1	0.07134	± 0.03551	0.12	0.3636	± 0.05004	0.002	0.009
	IgG	0.003162	± 0.001395		0.006713	± 0.0008975		
Akt1	DJ-1	0.04943	± 0.04827	0.8727	0.4395	± 0.04558	0.0007	0.0012
	IgG	0.0406	± 0.01766		0.001055	± 0.0004124		
Gapdh	DJ-1	0.08277	± 0.04203	0.4148	0.1354	± 0.07696	0.3	0.6
	IgG	0.04183	± 0.0162		0.04289	± 0.01952		

Figure S2: Statistical results of RNA-immunoprecipitation (RNA-IP) from WT and TSC cKO cortices. DJ-1 RNA-IPs were performed from a cortical lysates of either a WT or TSC cKO mice. RNA was isolated and quantitative RT-PCR was performed for *Cacna1c, Cacna2d2, Akt1*, and *Gapdh*. N= cortices isolated from 3 mice per genotype, students' t-test.

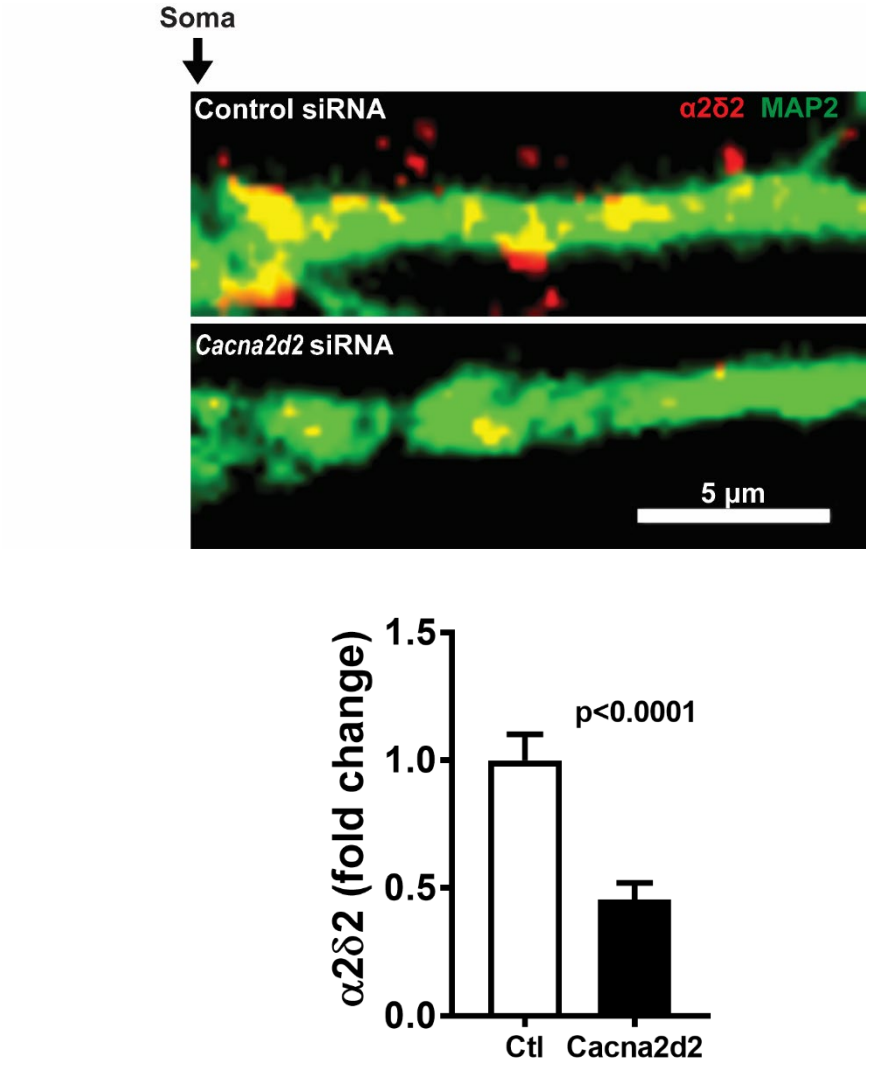

Figure S3: Verification of antibody against α2δ2. Cultured hippocampal rat neurons were transfected with a control or siRNA against α2δ2. Representative images are on top. Red/yellow puncta indicate α2δ2 staining in green dendrites. Note: fewer puncta detected in Cacna2d2 siRNA relative to control as quantified on the bottom. Statistical analyses: student's t-test, one-tailed; Control (Ctl) = 1 ± 0.1024, n=12; Cacna2d2 = 0.456 ± 0.06426, n=14; ****p <0.0001.

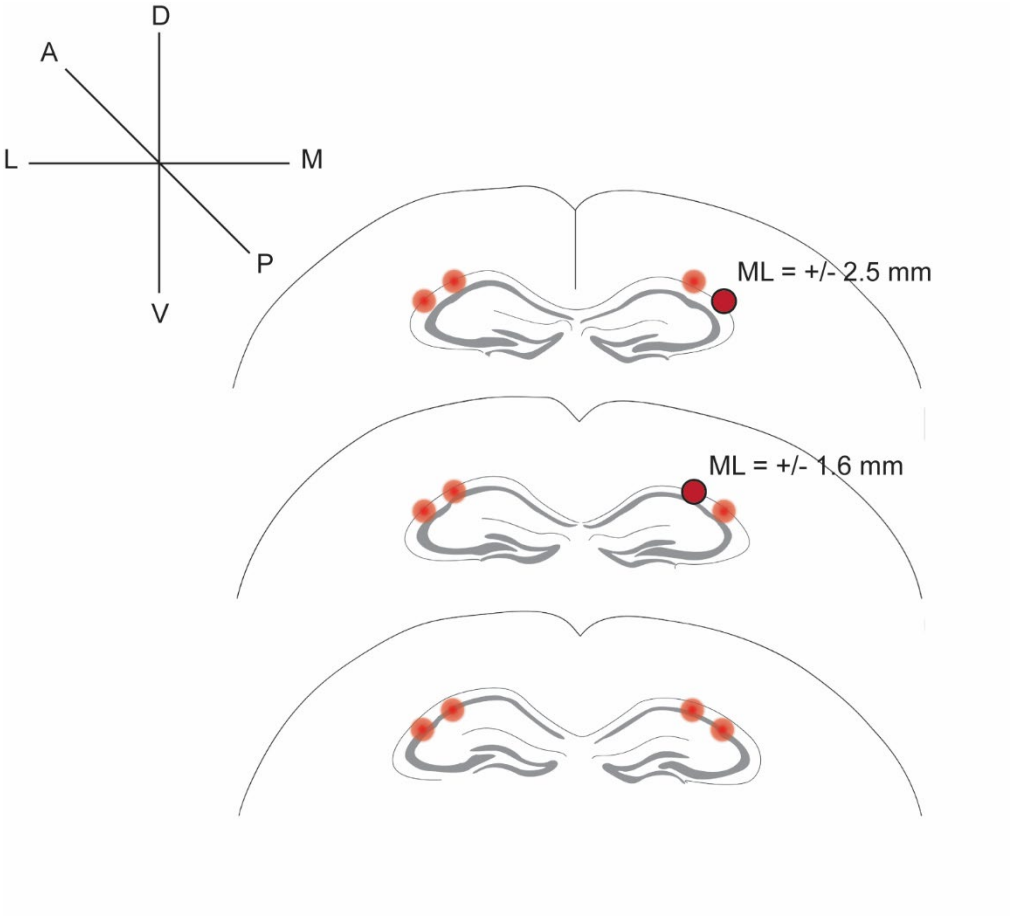

Figure S4: Schematic of stereotaxic injections of rAAV coding for DJ-1 and Cre recombinase. Mice were used in figures 2 and 3. Injection coordinates relative to bregma: 1) AP = -2.2 mm, ML = +/- 2.5 mm, and 2) AP = -2.5 mm, ML = +/- 1.6 mm; DV = -1.2, -1.1, -1.0. Adapted from "The Mouse Brain in Stereotaxic Coordinates" by Keith B. J. Frankin, and George Paxinos (2007).

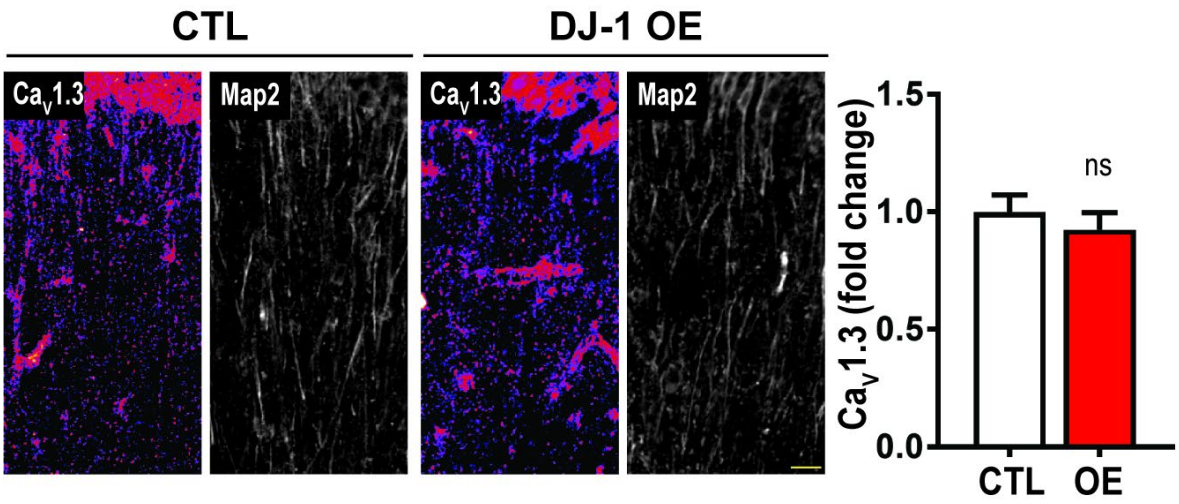

Figure S5: Cav1.3 expression doesn't change upon overexpression of DJ-1. CaV1.3 expression density is denoted by pseudo coloring (fire), and quantification (right), similar to Figure 3. Cav1.3/Map2 intensity ratio: CTL = 1 ± 0.07258; OE = 0.9242 ± 0.07255; two-tailed student's t-test; per condition = 5 ROI/slice, 1-2 slices/animal, 4 animals; p = 0.4653. Scale bar = 20µm.

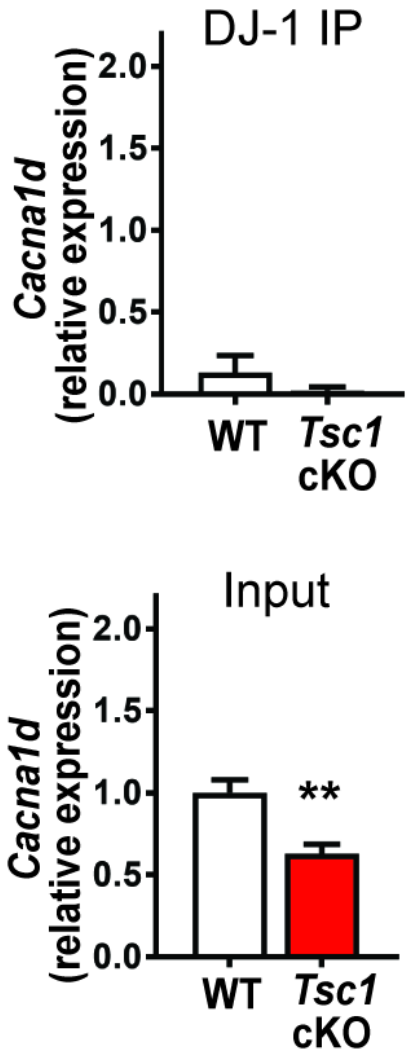

Figure S6: *Cacna1d* does not associate with DJ-1 in Tsc1 cKO mouse model. (*Top*) DJ-1 does not bind to Cacna1d as determined by RNA-IP using a specific antibody against DJ-1 followed by RNA isolation and quantitative RT-PCR. (Bottom) To determine relative expression levels of mRNA between genotypes RNA was isolated from 5% of the total input. There was a significant decrease in *Cacna1d* transcript levels in Tsc1 cKO cortical lysates. IP (top) WT = 0.13 ± 0.11, *Tsc1* cKO = 0.02 ± 0.02, p = 0.37. N= cortical lysates isolated from 3 mice/genotype. Statistical significance was determined by Students' t-test.

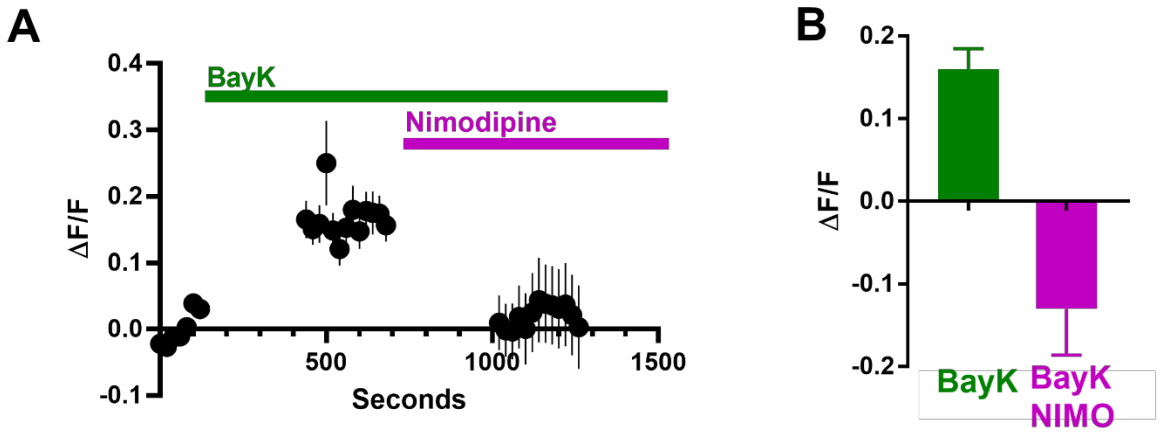

Figure. S7: L-type calcium activity in response to BayK and Nimodipine. Rat cultured hippocampal neurons were recorded for 140 second baseline. BayK (5uM) was added at 540 seconds followed by either vehicle or Nimodipine (1 μM) for 540 seconds. The relative change in L-type calcium activity as indicated by the following equation: $\Delta F/F= (F_t-F_0)/F_0$ where F0 for BayK was F for baseline, and F0 for BayK/Nimodipine was F for BayK, as determined for the bar graph in **B**. **p=0.0079, Students t-test, two-tail; n = 10 neurons, 24 dendrites.

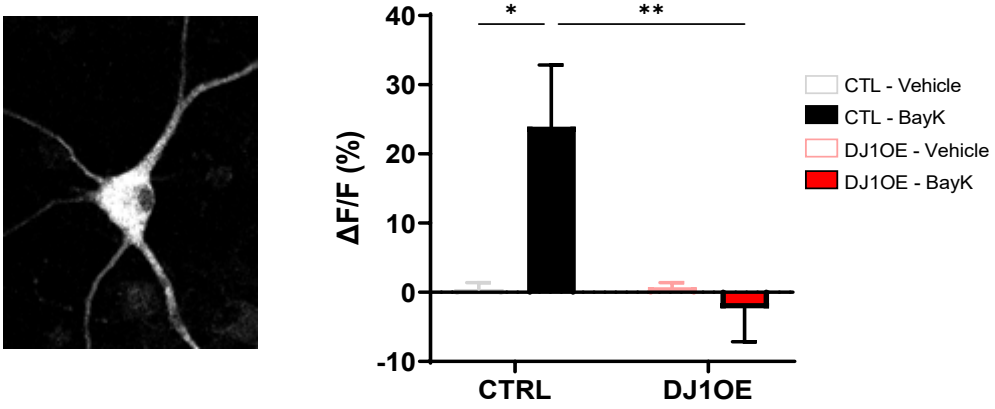

Figure S8: Utilization of GCaMP6-XC calcium indicator recapitulates that overexpression of DJ-1 reduces dendritic L-VGCC activity in response to BayK. *(Left)* Representative neuron transfected with GCaMPX6-XC. Scale bar = 25µm. *(Right)* Quantification of change in GCaMP6-XC signal (ΔF) normalized to baseline (F). Two-way ANOVA revealed a significant genotype x treatment interaction ($F_{1,101} = 4.851$, $p = 0.0299$). Tukey's multiple comparisons post hoc test revealed a significant difference between CTL-Vehicle (gray, 0.4997±0.8995, 23 dendrites, 7 neurons) vs. CTL-BayK (black, 23.9517±8.8899, 32 dendrites, 10 neurons), but no significant difference between DJ1OE-Vehicle (pink, 0.7379±0.6568, 24 dendrites, 8 neurons) vs. DJ1OE-BayK (red, -2.2923±4.8425, 26 dendrites, 8 neurons). Data was replicated in 4 independent cultures for each group. Statistics: 2-way ANOVA. Values represent mean ± SEM. *$p<0.05$, **$p<0.01$.

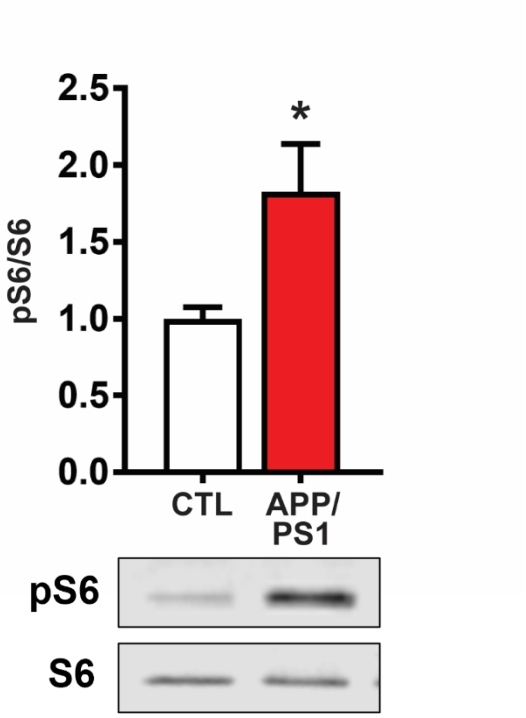

Figure S9. mTORC1 is overactive in APP/PS1 mouse model. WT = 1 ± 0.0736, n=9; APP/PS1 = 1.826 ± 0.3113, n=11; p = 0.0306; two-tailed student's t-test.

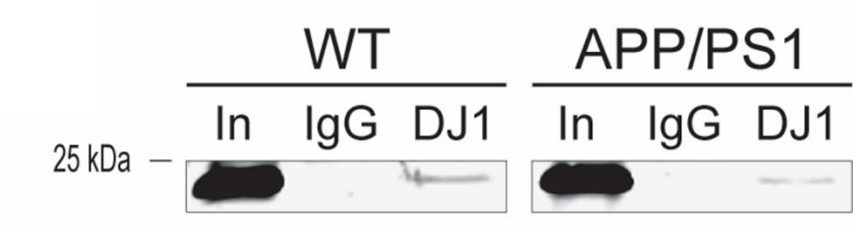

Figure S10. Western blot confirmation of RNA-Immunoprecipitation (R-IP) of DJ-1. Western blot of 25% of precipitate ran on 10% SDS-PAGE, showing DJ-1 is successfully immunoprecipitated from WT and APP/PS1 cortical lysates, while the negative control, IgG, is void of DJ-1 bands.

		WT			APP/PS1			WT vs APP/PS1 IP
		mean	SEM	p-value	mean	SEM	p-value	p-value
cacna1c	DJ-1	0.07077	± 0.02983	0.67	0.8701	± 0.1907	0.01	0.01
	IgG	0.05635	± 0.01201		0.06286	± 0.02257		
cacna2d2	DJ-1	0.07697	± 0.05363	0.8381	0.9506	± 0.2918	0.03	0.04
	IgG	0.06139	± 0.04724		0.05943	± 0.04614		
Akt1	DJ-1	0.02245	± 0.01041	0.33	0.6214	± 0.05569	0.0004	0.0005
	IgG	0.0092	± 0.006274		0.01007	± 0.005078		
Gapdh	DJ-1	0.2638	± 0.07874	0.36	0.3127	± 0.1006	0.22	0.72
	IgG	0.1557	± 0.07171		0.1619	± 0.02922		

Figure S11. Statistical results of RNA-immunoprecipitation (RNA-IP) from WT and APP/PS1 cortices. DJ-1 RNA-IPs were performed from a cortical lysates of either a WT or APP/PS1 mouse. RNA was isolated and quantitative RT-PCR of *Cacna1c*, *Cacna2d2*, *Akt1*, and *Gapdh* mRNA was performed. N=3 mice/genotype. Statistical significance was determined by students' t-test.

Case	Sex	Age	AP_PMI	Braak Stage	CERAD	Diagnosis
1	Female	93	4.58	V (B3)	Sparse (C1)	LOW AD
2	Male	90	4	VI (B3)	Frequent (C3)	HIGH AD
3	Male	91	5	III (B2)	No Plaques (C0)	No Dementia
4	Male	94	3.85	VI (B3)	Frequent (C3)	Dementia
5	Female	88	3.18	II (B1)	No Plaques (C0)	No Dementia
6	Female	70	5	VI (B3)	Frequent (C3)	Dementia
7	Female	98	2.25	I (B1)	No Plaques (C0)	No Dementia
8	Female	63	4.5	VI (B3)	Frequent (C3)	Dementia
9	Male	95	2.5	III (B2)	Sparse (C1)	Other
10	Male	87	5.5	V (B3)	Frequent (C3)	No Dementia

Figure S12. Characterization of Postmortem human tissue samples. Mean age of death is 86.9 years, and the postmortem interval (PMI) range average is 4.03 hours.

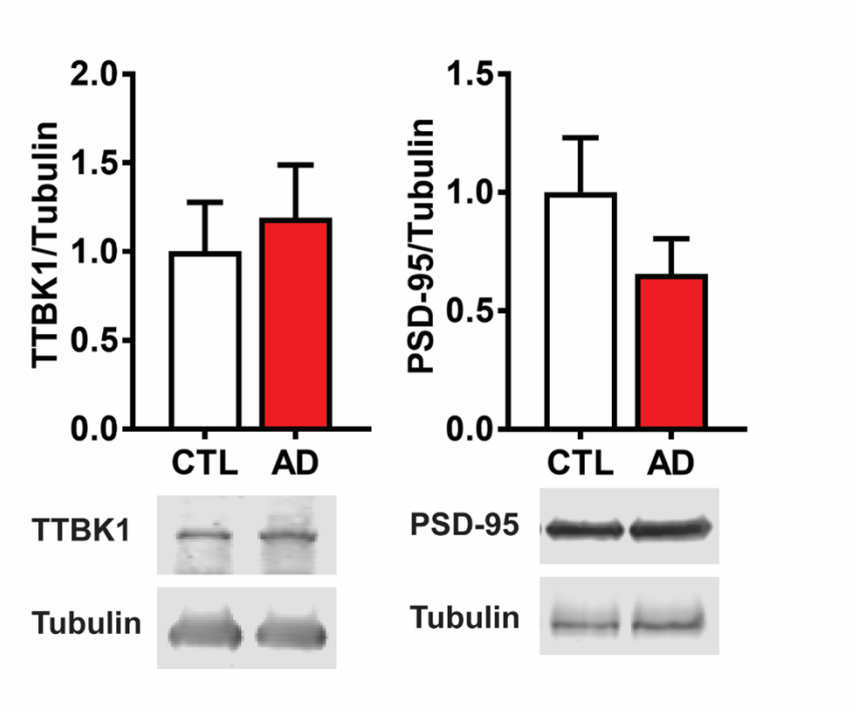

Figure S13: Control Western blot analyses of human PFC synaptoneurosomes. Amyloid precursor protein (APP, CTL = 1 ± 0.3855, n=5; AD = 1.135 ± 0.1657, n=5, p = 0.7552) , Tau-tubulin kinase 1 (TTBK1, CTL = 1 ± 0.2775, n=5; AD = 1.19 ± 0.2984, n=5) , and PSD-95 (CTL = 1 ± 0.2302, n=5; AD = 0.6546 ± 0.1499, n=5, p = 0.2440) expressions do not change in synaptoneurosomes isolated from AD patients compared to control patients.

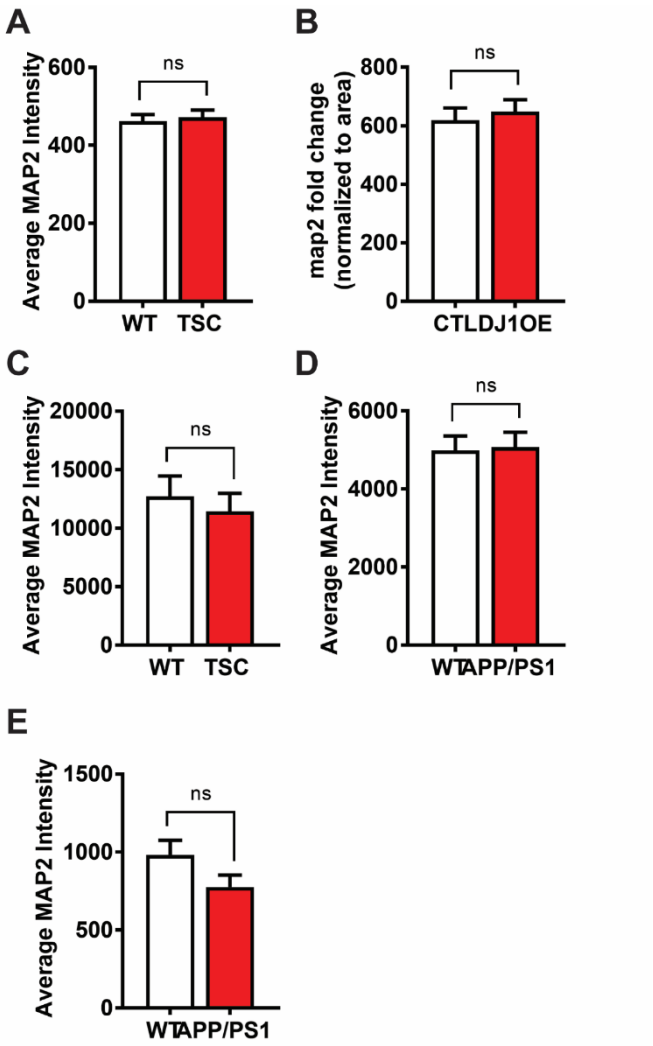

Figure. S14: Average Map2 intensity in primary neuronal cultures is comparable between genotypes or treatments. (A) Related to Figure 2A-C; quantification of average MAP2 intensity between WT (white, 12700 ± 1762, n= 356 dendrites, n=88 neurons, n=9 independent cultures) and TSCcKO (red, 11440 ± 1527, n=371 dendrites, n=85 neurons, n=9 independent cultures) hippocampal neuronal cultures. **B)** Related to figure 3A and 3B; DJ-1 overexpression (OE) (red, 619.2 ± 41.47, n=4) and WT (white, 648.3 ± 40.4, n=4) Map2 intensities are not significantly different. **(C)** Related to Figure 4A-C; quantification of average MAP2 intensity between WT (color, 461.2 ± 17.82, n= 153 regions of interest, n = 14 slices, n=9 independent mice) and TSCcKO (color, 471.7 ± 18.93, n= 160 regions of interest, n = 16 slices, n=9 independent mice) hippocampal acute slices. **(D)** Related to Figure 5A, 6A, 6B, and 6C; quantification of average MAP2 intensity between WT (white, 4988 ± 371.3, n= 295 dendrites, n=112 neurons, n=9 independent cultures) and APP/PS1 (color, 5071 ± 382.3, n= 283 dendrites, n=109 neurons, n=9 independent cultures) hippocampal neuronal cultures. **(E)** Related to Figure 5C; Quantification of average MAP2 intensity between WT (color, 4988 ± 371.3, n= 295 dendrites, n=112 neurons, n=9 independent cultures) and APP/PS1 (color, 5071

± 382.3, n= 283 dendrites, n=109 neurons, n=9 independent cultures) hippocampal neuronal cultures. Values represent mean ± SEM, student's t-test. n.s = no significance.

Supplemental Methods

Mouse models:

Tsc1 conditional knockout

Tsc1$^{fl/fl}$*Syn1-Cre*$^{+}$*:* Tsc1 cKO, and Tsc1 $^{fl/fl}$: WT mice were utilized for Figure 1 (1, 2). To generate Tsc1 cKO mice, homozygous, conditionally floxed Tsc1 (Tsc1^{tm1Djk}/J, Strain #: 005680, Jackson Laboratory) mice were crossed with mice bearing the Syn1-Cre allele (B6.Cg-Tg(Syn1-cre)671Jxm/J, Strain #: 003966 Jackson Laboratory), to generate homozygous (Tsc1$^{fl/fl}$ or Tsc1$^{fl/w}$, Tsc1 WT) and heterozygous mice for Tsc1 (Tsc1$^{fl/w}$Syn1-Cre^{+}, Tsc1 HET). Here, fl and w denote the conditional (floxed), and wild-type alleles of Tsc1, respectively, and + designates the presence of the aforementioned allele. A second cross between Tsc1$^{fl/w}$Syn1-Cre+ and Tsc1$^{fl/fl}$ was performed to generate Tsc1$^{fl/fl}$Syn1-Cre^{-} (Tsc1 WT), Tsc1$^{fl/w}$Syn1-Cre^{-} (Tsc1 WT), Tsc1$^{fl/w}$Syn1-Cre^{+} (Tsc1 HET), and Tsc1$^{fl/fl}$Syn1-Cre^{+} (Tsc1 KO) mice. For the other experiments using TSC mouse model, *Tsc1^{tm1Djk}*/J mice (Jackson Laboratory, Bar Harbor, ME) were used for *in vivo* and *in vitro* experiments (1). Both AAV-GFP (AAV5-hSyn-eGFP 4 x 10^{12} GC/mL) and AAV-CRE-GFP (AAV5-hSyn-CRE-eGFP 5 x 10^{12} GC/mL) were driven by a synapsin promoter. As previously described for *in vivo* studies, AAV-Cre-GFP or AAV-GFP were injected into the hippocampus of 7 to 8 weeks-old male mice using the following coordinates (from bregma): ±2.2 mm A/P, ±1.5 mm M/L; ±2.5 mm A/P, and ±1.6 mm M/L (Fig. S3) (3).

APP/PS1

The APP/PS1 mouse line is used as a preclinical model for AD, which expresses human/murine amyloid precursor protein (APP) construct containing the Swedish double mutation (APPswe) and presenilin (PSEN1 or PS1) construct without the exon 9 (PSEN1/ΔE9)

Identification of DJ-1 binding motif(s)

Using a 45-nucleotide consensus sequence previously identified, we constructed a list of all possible 6-12 nucleotide substrings, a typical length of RNA-binding motifs (4-7). Each substring was then ranked based on the sum of its probability values based on the probabilities derived from the consensus logo. We found that two motifs GNGCNG or CNGCNG occurred with highest probability. To find the frequency of occurrences for these motifs in a given DNA alphabet, we used the seqinr and Biostrings packages (8, 9). The graphical user interface for this process was developed using the shiny package in R along with the DT package (10, 11). Postsynaptic proteome/gene data were obtained from Collins et al (2006) and Bayes et al (2012) available online at G2C: Genes to Cognition database (http://www.genes2cognition.org/) (12, 13). All gene sequences were obtained using the biomart package (14-16). Within the 5' UTR, CR (coding region), and 3' UTR sequences of the 1,416 postsynaptic genes with available sequence data were searched for DJ-1 RNA-binding motifs (GNGCNG or CNGCNG). R Script for determining the number of DJ-1 binding is deposited at

https://github.com/snamjoshi/niere_uneri_etal_2022 [github.com]. All matches were then filtered to obtain only the maximum length sequences, and the total number of DJ-1 binding sites for each gene was calculated. To test the specificity of the predicted DJ-1 binding sites, we determined the frequency of DJ-1 binding sites per kB of the mRNA sequence of each PSD-associated protein provided in Bayes et al (2012)(13). We then compared the frequency/kB of DJ-1 binding sites between putative DJ-1-targets and non-targets to determine that DJ-1 target mRNAs significantly express more DJ-1-binding sequences than non-targets. These data were thresholded using *Grin2A* as a cutoff (Dataset S1), as *Grin2A* is a common disease-associated protein shared by diseases with dysregulated mTOR described by Niere *et al*. 2016 (3).

Cultured Neurons

Both male and female mice were used, and WT littermates served as control for studies involving APP/PS1. Briefly, hippocampi were extracted from postnatal day 1–3 *Tsc1*^{tm1Djk}/J or APP/PS1 mouse pups. The tissue was dissociated and plated in neurobasal A medium supplemented with B27, glutamine, and 1% fetal bovine serum. Cultures were plated at a density of ~100,000 cells per 12 mm on glass coverslips that had been coated overnight with 50 μg ml^{-1} poly-D-lysine and 25 μg ml^{-1} laminin in borate buffer. Cultures were fed after 1 day after plating, and media was replaced approximately once a week with either fresh rat culture media (neurobasal A supplemented with B27, glutamine and 3 μM cytosine arabinoside (AraC)) or fresh mouse culture media (glial-conditioned media with 3 μM AraC) until cultures were used at DIV 14–21.

Fluorescence in Situ Hybridization

Briefly, primary hippocampal neurons (days *in vitro* (DIV) 20-21) were fixed at room temperature for 30 minutes with a 4% paraformaldehyde solution (4% paraformaldehyde, 5.4% glucose, 0.01M sodium metaperiodate, in lysine-phosphate buffer). Proteinase K treatment was omitted and the rest of the hybridization was completed according to the manufacturer's instructions. The cells were then washed with PBS and blocked with 4% goat serum in PBS for one hour followed by incubation in primary antibody (chicken anti-GFP) overnight at 4°C. After three washes with PBS the cells were incubated with the appropriate secondary antibody for one hour at room temperature and washed with PBS. The coverslips were then mounted with an antifading mounting medium and imaged as described above.

RNA-Immunoprecipitation (RIP)

Mouse cortical tissue (pooled from 2 mice) was homogenized in PLB buffer (10mM Hepes pH 7.0, 100 mM KCl, 25 mM EDTA, 5 mM MgCl2, 1mM DTT and 0.5% NP-40) and incubated for 10 minutes on ice. The samples were then centrifuged for 14,000 xg for 15 minutes at 4°C. Protein concentration of the supernatant was determined with a BCA assay to ensure equal concentrations of starting material was used. The supernatant was then precleared with 5 µg mouse IgG and 100 µl of Dynabeads (Protein G, Thermo) for 30 minutes at 4°C. Beads washed with NT2 buffer (50 mM Tris-HCl pH 7.4, 150 mM NaCl, 1 mM MgCl2, 1mM DTT, 0.05% NP-40 with Halt™

Protease Inhibitor Cocktail (Thermo Scientific)) were incubated with either 30 µg DJ-1 antibody (Santa Cruz) or mouse IgG (Santa Cruz) for 1 hour at 4°C. The beads were washed 3 times with NT2 buffer. The precleared samples (5 mg) were incubated with the conjugated beads overnight at 4°C. The beads were washed 4 times with NT2 buffer and were suspended in 100 µl NT2 buffer. 25 µl of the bead suspension was removed and 2X Laemmli sample buffer (BioRad) containing β-ME was added. Western blot analysis was used to confirm DJ-1 immunoprecipitation. The remaining sample was used for RNA extraction following the instructions from the Absolutely RNA Nanoprep Kit (Agilent). RNA was resuspended in molecular grade water.

RT-qPCR

qPCR was performed in triplicate for each transcript isolated from 3 independent mice. For the standard curve, total RNA was extracted with Trizol from mouse cortical tissue, and reverse transcribed as outlined according to the manufacturer's directions, starting from 1ug of total RNA (TakaraBio cDNA synthesis kit). The standard curve for each transcript was established by using a 4-fold serial dilution of cDNA. For RIP, reverse transcription was performed using SMARTer cDNA synthesis kit (TakaraBio), according to the manufacturer's instructions with total RNA isolated from RIP. qPCR amplification was performed using SsoAdvanced Universal SYBR® Green Supermix, with CFX Opus 96 Real Time PCR system (BioRad), with gene specific primers for *Cacna1c* (5'- GCTGTGTTACTGCTGTTCAGG -3', antisense 5'-TGAGAGATGTCTCCCCCTTGAT -3'), *Cacna1d* (5'-CGGAACAAGAACAGCGACAA-3', antisense 5'-CTGGCAGCACTTTCCATCTC-3'), Cacna2d2 (5'-

ACGCCCGCTCTTGCTCTTGCT-3', antisense 5'- CCTCCAAAAATCCGCATCAC -3'), *Cacna2d1* (5'- GACCTTGTCACACTGGCAAA-3', antisense 5'-GGCTGCTTGGACTTTCTCTG-3'), *Akt1* (5'-TCCTCAAGAACGATGGCACC-3', antisense 5'- CTGCAGGCAGCGGATGATAA -3'), and *Gapdh* (5'-GGTGCTGAGTATGTCGTGGA-3', antisense 5'-CCTTCCACAATGCCAAAGTT-3'). To determine the quantity of RNA that binds to DJ-1 or IgG, we used the equation $10^{[(Ct-b)/m]}$, where m is the slope and b is the y-intercept of the standard curve. The quantity was the average of the three replicates, and was normalized to WT input, yielding the relative expression (17).

Surface Sensing and Translation– Proximity Ligation Assay (SUnSET-PLA)

400 µm transverse hippocampal sections were prepare with a Leica VT1200S vibratome. Sections were maintained in room temperature aCSF for 2 hours. aCSF contained 118 mM NaCl, 3.5 mM KCl, 2.5 mM CaCl2, 1.3 mM MgSO4, 1.25 mM NaH2PO4, 5 mM NaHCO3, 15 mM glucose and was bubbled with 95% O2/5% CO2. Sections were then treated with 0.5ug/ml puromycin for 1 hour in oxygenated aCSF at 32°C. Following treatment, the CA1 region of the hippocampus was microdissected and then fixed overnight with 4% paraformaldehyde (PFA). After fixation, 400µm slices were resectioned to 60µm sections using a vibratome. 60µm hippocampal sections were first washed in 1XPBS with + 0.75% glycine 3 times for 10 minutes. Sections were then permeabilized and blocked (10% normal donkey serum (NDS), 0.25% Tween-20, and 1XPBS) for 2 hours at room temperature. After blocking, sections incubated overnight in primary antibodies at 4°C in blocking solution. Sections were washed in 1XPBS/glycine

3 times for 10 minutes, and then incubated in secondary antibodies for 2 hours at 37°C. Primary antibodies used for PLA: mouse anti-puromycin (1:150, Millipore Sigma), rabbit anti-$Ca_V1.2$ (1:150, Alomone Labs), rabbit anti-a2d2 (1:150, Novus Biologicals; verification Fig. S2), and rabbit anti-α2δ1 (1:150, Alomone Labs). Primary antibodies used for immunohistochemistry: chicken anti-MAP2 (1:1,000, Abcam). PLA detection of puromycin and specific calcium channel subunit was performed according to the manufacturer instructions (Millipore Sigma, DUO82409). Secondary antibodies used for PLA: donkey anti-rabbit PLUS (1:5, DUO92002), donkey anti-mouse MINUS (1:5, DUO92001). Secondary antibody used for immunohistochemistry: donkey anti-chicken 488 (1:400, Life Technologies).

Immunofluorescence

For hippocampal slices, mice were transcardially perfused with phosphate buffered saline (0.1 M). Brains were removed and postfixed in 4% paraformaldehyde. 50 μm thick slices were prepared and checked for GFP/RFP expression, depending on the experiment. Slices expressing fluorescent protein were processed for IHC, similar to Niere *et al*, using the following primary antibodies: rabbit anti-α2δ2 (1:150, Novus Biologicals), rabbit anti-$Ca_V1.2$ (1:150; Alomone Labs), rabbit anti-α2δ1 (1:150; Alomone Labs), mouse anti-MAP2 (1:500, Abcam), and chicken anti-GFP (1:500, Aves) (18). With dissociated hippocampal neurons, cells were fixed in 4% paraformaldehyde for 20 minutes at room temperature and permeabilized in 0.2% Triton X-100 for 10 minutes (18). Fixed cells were incubated overnight in 4°C with the following primary antibodies: rabbit anti-α2δ2 (1:500, Novus Biologicals) or rabbit anti-DJ-1 (1:1000,

Novus Biologicals), and chicken anti-Map2 (1:1000, Aves) or mouse anti-Map2 (1:1000, Abcam). Appropriate secondary antibodies (1:500, Life Technologies) were used—AlexaFluor488 (AF488), AF647, AF405—after overnight primary antibody incubation.

Synaptoneurosome preparation

Tissues were harvested from patients that were clinically diagnosed with AD, where the neuropathology of AD was confirmed and from controls who exhibited low levels of AD neuropathology. The samples in this study underwent rapid autopsy shortly after death, where the harvested tissue was flash frozen. Samples from AD and CTL patients were prepared blinded as to condition. Frozen postmortem human prefrontal cortex samples from UW Neuropathology Core were homogenized with a buffer composed of Tris-Base with Halt™ Phosphatase and Protease Inhibitor Cocktail (Thermo Scientific). Homogenates were then sequentially filtered through 100µm cell strainer and 5µm syringe filter and centrifuged for 20 minutes in 4°C at 14,000 xg. The pellet was solubilized with RIPA buffer and centrifuged for 10 minutes in 4°C at 14,000 xg. The supernatant was collected for protein quantification using Pierce™ BCA Protein Assay Kit (Thermo Scientific).

Western blot analysis

Samples were prepared into SDS-polyacrylamide gel electrophoresis (PAGE) loading buffer using 4x Laemmli Sample Buffer (Bio-Rad). 50 µg protein from each sample were resolved in 10% SDS-polyacrylamide gel and transferred onto 0.2 µm nitrocellulose

membranes (Bio-Rad). The nitrocellulose membranes were blocked in 5% nonfat dry milk in Tris-buffered saline containing 0.1% Tween 20. To visualize the proteins, we used: mouse anti-DJ1 (1:2000; Novus Biologicals), mouse anti-tubulin (1:20,000; Abcam), rabbit anti-α2δ2 (1:5000; Alomone Labs), mouse anti-$Ca_V1.2$ (1:1000; Neuromab). Antibody-bound membranes were incubated in fluorescence-conjugated secondary antibodies (AF680, Life Technologies; AF800, LiCor; 1:5000). Fluorescent images of the membranes were obtained using the Odyssey CLx infrared imaging system. Densitometry analyses of proteins were conducted using ImageJ (National Institutes of Health) software.

Calcium imaging

Cells were then transferred to fresh ACSF (37°C) for imaging (1 frame per 2 0 seconds). Baseline calcium signal was imaged (1 minute), after which BayK-8644 (5 µM, Tocris) or vehicle (DMSO) was added. Neurons were imaged for ~600 s at room temperature. Quantification of the calcium signal was performed using Metamorph (Molecular Devices). Briefly, dendritic regions of interest (ROI) that were at least 5 µm from the soma were analyzed. The mean intensity values for each ROI at every 20 seconds were averaged as baseline (F_0). The ROI intensity values obtained at each time point after the addition of BayK-8644 or vehicle were averaged (F). For the genetically encoded calcium indicator, we used AAV-syn-GCaMP6m-XC, from Xiaodong Liu (Addgene plasmid # 118975) (19). The adeno-associated viral (rAAV) particles for GCamp6-XC sensor were produced by cotransfecting 293FT cells with the plasmids of AAV-syn-GCaMP6m-XC, pAAV2/9n (Addgene #112865) and

pAdDeltaF6 (Addgene #112867). The transfection, viral collection and purification in AAV production were following the methods as described previously (20). GCaMP6-XC virus was added directly to the neuronal culture media on DIV10. On DIV14, neurons were imaged for GCaMP6-XC fluorescence (1 frame per 5 seconds). Prior to imaging, cells were transferred from media to freshly prepared ACSF. Baseline signal was imaged (1 minute), after which BayK-8644 (5μM, Tocris) or vehicle (DMSO) was added. Neurons were imaged for 540 seconds at room temperature. Quantification of dendritic GCaMP6-XC signal was analyzed in regions of interest (ROI) at least 5μm from the soma. The mean intensity values for each ROI at every 5 seconds were averaged as baseline (F0). The ROI intensity values obtained at each time point after the addition of BayK-8644 or vehicle were averaged (F). The equation, $\Delta F/F=((F-F0)/F0)$, was used to measure the change in signal.

References:

1. D. J. Kwiatkowski *et al.*, A mouse model of TSC1 reveals sex-dependent lethality from liver hemangiomas, and up-regulation of p70S6 kinase activity in Tsc1 null cells. *Human molecular genetics* **11**, 525-534 (2002).
2. L. Meikle *et al.*, A mouse model of tuberous sclerosis: neuronal loss of Tsc1 causes dysplastic and ectopic neurons, reduced myelination, seizure activity, and limited survival. *J Neurosci* **27**, 5546-5558 (2007).
3. F. Niere *et al.*, Analysis of Proteins That Rapidly Change Upon Mechanistic/Mammalian Target of Rapamycin Complex 1 (mTORC1) Repression Identifies Parkinson Protein 7 (PARK7) as a Novel Protein Aberrantly Expressed in Tuberous Sclerosis Complex (TSC). *Molecular & cellular proteomics : MCP* **15**, 426-444 (2016).
4. M. P. van der Brug *et al.*, RNA binding activity of the recessive parkinsonism protein DJ-1 supports involvement in multiple cellular pathways. *Proceedings of the National Academy of Sciences of the United States of America* **105**, 10244-10249 (2008).
5. L. P. Benoit Bouvrette, S. Bovaird, M. Blanchette, E. Lecuyer, oRNAment: a database of putative RNA binding protein target sites in the transcriptomes of model species. *Nucleic acids research* **48**, D166-D173 (2020).
6. D. Dominguez *et al.*, Sequence, Structure, and Context Preferences of Human RNA Binding Proteins. *Molecular cell* **70**, 854-867 e859 (2018).
7. X. Li, H. Kazan, H. D. Lipshitz, Q. D. Morris, Finding the target sites of RNA-binding proteins. *Wiley interdisciplinary reviews. RNA* **5**, 111-130 (2014).
8. D. Charif, J. R. Lobry, "SeqinR 1.0-2: A Contributed Package to the R Project for Statistical Computing Devoted to Biological Sequences Retrieval and Analysis" in Structural Approaches to Sequence Evolution, U. Bastolla, M. Porto, H. E. Roman, V. M, Eds. (Springer, Berlin ; New York, 2007), https://doi.org/10.1007/978-3-540-35306-5_10, pp. xix, 367 p.
9. H. Pages, P. Aboyoun, R. Gentleman, S. Debroy, Biostrings: String objects representing biological sequences, and matching algorithms. *R package version 2.42.1* (2016).
10. W. Chang, J. Cheng, J. J. Allaire, Y. Xie, J. Mcpherson, shiny: Web Application Framework for R. *R package version 0.14.2* (2016).
11. Y. Xie, DT: A Wrapper of the JavaScript Library 'DataTables'. *R package version 0.2* (2016).
12. M. O. Collins *et al.*, Molecular characterization and comparison of the components and multiprotein complexes in the postsynaptic proteome. *J Neurochem* **97 Suppl 1**, 16-23 (2006).
13. A. Bayes *et al.*, Comparative study of human and mouse postsynaptic proteomes finds high compositional conservation and abundance differences for key synaptic proteins. *PloS one* **7**, e46683 (2012).
14. S. Durinck *et al.*, BioMart and Bioconductor: a powerful link between biological databases and microarray data analysis. *Bioinformatics* **21**, 3439-3440 (2005).
15. S. Durinck, P. T. Spellman, E. Birney, W. Huber, Mapping identifiers for the integration of genomic datasets with the R/Bioconductor package biomaRt. *Nature protocols* **4**, 1184-1191 (2009).
16. D. Smedley *et al.*, The BioMart community portal: an innovative alternative to large, centralized data repositories. *Nucleic acids research* **43**, W589-598 (2015).
17. J. M. Gallup, M. R. Ackermann, The 'PREXCEL-Q Method' for qPCR. *Int J Biomed Sci* **4**, 273-293 (2008).
18. F. Niere, J. R. Wilkerson, K. M. Huber, Evidence for a fragile X mental retardation protein-mediated translational switch in metabotropic glutamate receptor-triggered Arc translation and long-term depression. *J Neurosci* **32**, 5924-5936 (2012).

19. Y. Yang *et al.*, Improved calcium sensor GCaMP-X overcomes the calcium channel perturbations induced by the calmodulin in GCaMP. *Nat Commun* **9**, 1504 (2018).
20. T. Kimura *et al.*, Production of adeno-associated virus vectors for in vitro and in vivo applications. *Sci Rep* **9**, 13601 (2019).